Influence of secondary decay on isotope-ratio temperature measurements

H. Xi, W. G. Lynch, and M. B. Tsang

National Superconducting Cyclotron Laboratory, Michigan State University, East Lansing, Michigan 48824

W. A. Friedman

Department of Physics, University of Wisconsin, Madison, Wisconsin 53706

D. Durand

Laboratoire de Physique Corpusculaire, Caen, F-14050 Caen Cedex, France

Influence of sequential decay on nuclear temperature measurements is studied. Particular attention is paid to the contribution of higher-energy resonances and to the role of the primary charge distribution. Results of calculations show that temperatures extracted from the measured double isotope ratios are strongly affected at temperatures beyond 6 MeV. The fluctuations between different isotope thermometers observed in the experiment seem mainly due to structure effects in the secondary decay process. [S0556-2813(99)04603-8]

I. INTRODUCTION

In intermediate-energy heavy-ion collisions, nuclear fragments are emitted from highly excited systems. Production of these particles appears to be dominated by their phase space, and can be described by statistical physics. Thus, temperature, a basic quantity in statistical physics, can be addressed experimentally. Two methods have been most commonly used to measure nuclear temperatures, both of which assume thermal and chemical equilibrium at a single freeze-out condition. One method is to measure the yields of particle unstable states [1–9]. Another method is based on the double ratio of two isotope pairs [10–16].

Nuclear temperature has been studied extensively in the last decade. Most work has focused on the measurement of excited states yields [1–9], where temperature is deduced from the yields of two states in one isotope

$$T = \frac{E_1 - E_2}{\ln(a' Y_1 / Y_2)}. \tag{1}$$

Here $a' = (2J_2 + 1)/(2J_1 + 1)$, E_i is the excitation energy, Y_i is the measured yield, and J_i is the spin factor of the state i. Experimental results show that temperature extracted from Eq. (1) increases slowly from 3 to 6 MeV over a large range of incident energy [7].

Recently, nuclear temperatures also have been studied using double isotope yield-ratios [10]. Yields of two pairs of isotope, each with one neutron difference, are measured and temperature is defined as

$$T = \frac{B}{\ln[a(Y_1 / Y_2)/(Y_3 / Y_4)]}, \tag{2}$$

where Y_1, Y_2 are the yields of one isotope pair and Y_3, Y_4 is another isotope pair; B is the binding energy difference $B = BE_1 - BE_2 - (BE_3 - BE_4)$. Here, the statistical weighting factor a is defined as

$$a = \frac{(2S_3 + 1)/(2S_4 + 1)}{(2S_1 + 1)/(2S_2 + 1)} \left[\frac{A_3 / A_4}{A_1 / A_2} \right]^{1.5}, \tag{3}$$

where S_i is the ground state spin factor and A_i is the mass number of the isotope i. The mass factors arise from the integration over phase space volume.

For Au+Au collisions at $E/A = 600$ MeV [11], the deduced temperature $T_{\text{HeLi}} = 13.32/\ln(2.18 R_{\text{HeLi}})$ from the double ratio of $R_{\text{HeLi}} = [Y(^6\text{Li})/Y(^7\text{Li})]/[Y(^3\text{He})/Y(^4\text{He})]$ remains relatively constant as a function of deduced excitation energy for $2.5 \text{ MeV} \leq E^*/A \leq 10 \text{ MeV}$, but increases rapidly at $E^*/A \geq 10$ MeV [11]. This trend resembles a first order liquid gas phase transition. This observation is different from the slow increase of temperature with incident energy as observed in inclusive experiments that measured excited state population. Recently, temperatures have been measured both from excited states population and double isotope ratios for Au+Au central collision from $E/A = 50$ to 200 MeV. Apparent temperatures deduced from excited state populations are independent of incident energy. In the same experiments, apparent temperatures from double isotope ratios constructed with $Y(^3\text{He})/Y(^4\text{He})$ ratios increase more rapidly with beam energy [12]. At the lowest beam energy, the two thermometers are close to each other.

Temperatures from ten isotope ratios ''all involving $Y(^3\text{He})/Y(^4\text{He})$ yield-ratios'' have been obtained for $35A$ MeV Au+Au central collisions [13]. The apparent temperatures depend on the specific pairs. This variation among different isotope thermometers is also observed in Ar+Ni at $95A$ MeV for a wide range of excitation energy [14]. Because the primary fragments produced in the reaction at freeze-out stage are normally highly excited, they will undergo secondary decays. Thus, the measured yields used to construct the apparent temperature are different from distributions of the ground state populations at the freeze-out stage. This sequential decay effect may account for the observed difference between different thermometers.

In an attempt to include the secondary decay effect, temperatures deduced from R_{HeLi} were multiplied by 1.2 in Ref.

[11]. This scaling factor was obtained from the quantum statistical model (QSM) [17] by comparing temperatures deduced from R_{HeLi} to the model temperature. It, however, depends on the model parameters [11,12,16–19]. Furthermore, in this model, only fragments in known bound states and resonances are taken into account. It neglects contributions from higher resonances that are important especially when the fragments are highly excited.

In this work, we study the influence of secondary decay on nuclear temperature derived from excited states population and double isotope ratios using a model which is described in Sec. II. In Sec. III, we discuss effects of the experimental constraints imposed on the model. In Sec. IV, the fluctuations among different isotope temperatures will be discussed. Finally, a summary will be given in Sec. V.

II. SEQUENTIAL DECAY MODEL

Highly excited nuclear systems formed in heavy-ion reactions will deexcite by emitting nuclear fragments. In general, these emitted fragments are themselves excited and will deexcite by emitting particles and gamma rays to the final ground states. To address questions relating to the temperature of the nuclear system, we describe the two stages of emission with the model first developed in Refs. [3–6]. In the first stage, the excited system emits fragments in their ground and excited states according to a statistical description; possible candidates for this description range from the evaporation from a heavy residue to the complete vaporization of the system. In the second stage, the excited fragments produced in the first stage decay to the ground states.

A. Initial fragment populations

Assuming emission from a composite system of mass number A_0 and charge number Z_0 we approximate the initial population of a given excited state by the expression

$$P(N_i, Z_i, E_i^*, J_i, \mu_p, \mu_n, T_{em})$$

$$= C(2J_i+1)(N_i+Z_i)^{1.5} \exp\left(-\frac{V_i}{T_{em}} + \frac{Q_i}{T_{em}}\right)$$

$$\times \exp\left(-\frac{E_i^*}{T_{em}}\right) \exp\left(-\frac{Z_i\mu_p + N_i\mu_n}{T_{em}}\right) P(t_b/t_i). \quad (4)$$

The excited state is characterized by, excitation energy E_i^*, spin J_i, neutron number N_i, and charge number Z_i while V_i is the Coulomb barrier, $-Q_i$ is the separation energy for emission of this nuclear state from the residue. T_{em} is the emission temperature or the temperature at freeze-out. The "chemical potentials" μ_p and μ_n, are treated as free parameters to reproduce both the experimental (final) charge distributions, and the charge-to-mass ratios of the emitted charged particles up to $Z=13$ as will be discussed in Sec. III. The suppression factor $P(t_b/t_i)$ will be discussed in the next subsection. While Eq. (4) does not correspond directly to either the limit of evaporation [20,21] or of bulk multifragmentation [22,23], it can approach those limits for suitable choices of μ_n and μ_p.
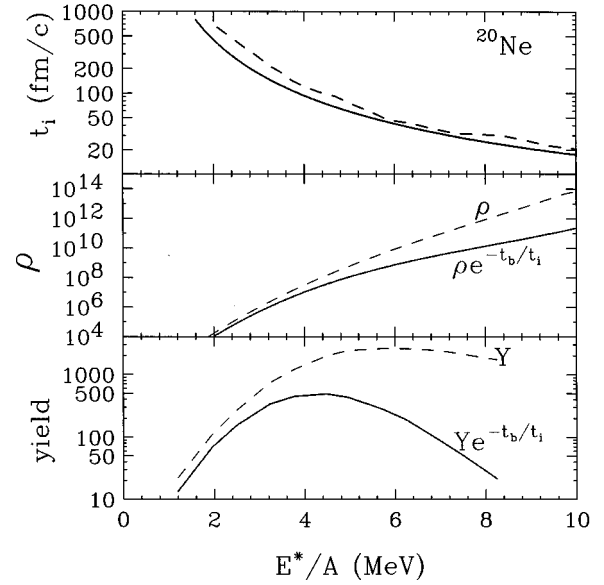

FIG. 1. Lifetime (top panel), level density (middle panel), and yield (bottom panel) as a function of the excitation energy of ^{20}Ne. In the middle and bottom panels, the solid lines represent level density and yield after the suppression factor $\exp(-t_b/t_i)$ is included.

B. Decay of excited fragments

Each decay from the initial excited fragment is calculated using tabulated branching ratios when available [3–6,24], or by using the Hauser-Feshbach formalism [25], when such information is unavailable. The model includes all experimentally known discrete bound states and resonant states for nuclei with charge less than or equal to 13. Unknown spins and parities of tabulated resonant states were randomly assigned in these calculations [3–6] and then changed in subsequent calculations to assess the corresponding uncertainties. In general, the uncertainties in isotope ratio calculation, due to the uncertainties in the unknown spins and parities are of the order of 5%.

When the excitation energy is high, the calculations must consider decays from short-lived unidentified states with no barrier to particle emission. These states are included in the model by using the Fermi-gas level density formula in Ref. [26]. In this article, the contributions from these states will be referred to as the "continuum." These continuum states are matched to the known discrete states for any given isotope as described in Refs. [3–6].

For the very short-lived states, it is likely that the states will decay before the excited fragments are fully separated from each other. The solid line in the top panel of Fig. 1 shows the relationship between the lifetime t_i and excitation energy for ^{20}Ne using the Weisskopf model [20]

$$t_i = \hbar/\Gamma, \quad (5)$$

where $\hbar = h/2\pi$ and h is the Planck's constant and the decay width Γ was calculated as in Ref. [21],
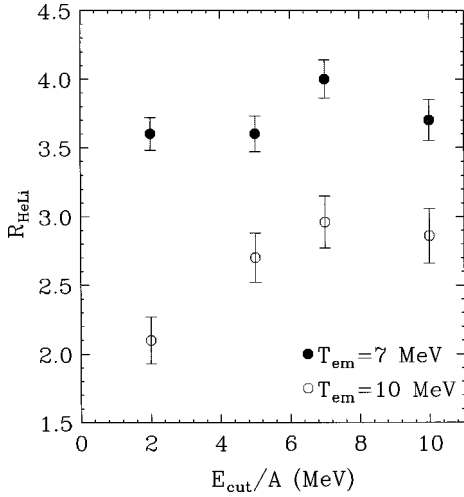
$$\Gamma \propto \sum_i T^2 e^{-V_i/T} F_i(T). \quad (6)$$

FIG. 2. Effect of the cutoff energy to the double isotope ratio R_{HeLi} for two calculations $T_{em}=7$ MeV (closed points) and 10 MeV (open points).

FIG. 3. Calculated T_{HeLi} as a function of input temperatures T_{em} by including different excited states.

The summation is over particles types $n,p,d,t,^3$He,^{4}He. F_i is the temperature-dependent free energy and V_i is the emission barrier of particle i. T is the temperature calculated from excitation energy using Fermi gas formula $T=\sqrt{E^*(8/A)}$ MeV. The prediction is nearly identical to the calculations (dashed line) from the Feshbach formula [25], where the branching ratios were taken from tabulated tables [24]. As shown in Fig. 1, the lifetime decreases dramatically with excitation energy. Above $E^*/A=5$ MeV, the lifetime is less than 50 fm/c.

To take this prebreakup effect into account, a suppression factor, $P(t_b/t_i)=\exp(-t_b/t_i)$ is included in Eq. (1). In the present work, we chose the parameter t_b to be 100 fm/c, a typical breakup time for multifragmentation process [27]. To illustrate the effect of the lifetime suppression factor, the level density, number of levels per MeV of excitation energy, was plotted in the middle panel of Fig. 1 as a function of the excitation energy per nucleon of ^{20}Ne. The dashed line is the level density calculated from the Fermi gas model [26] and the solid line is the effective level density $\rho(E^*)\exp(-t_b/t_i)$. The Fermi gas level density increases rapidly with excitation energy while the effective level density increases much slower especially at high excitation energy. The slower increase of the level density agrees with the trend from the shell model calculations of Mustafa which only take stable and metastable states into consideration [28].

The bottom panel of Fig. 1 shows the relative yields of ^{20}Ne excited states as a function of excitation energy assuming $T_{em}=8$ MeV. Since the yield is not normalized to a particular set of experimental data, it is plotted in arbitrary units. With no level density suppression (dashed lines), the yield increases and flattens out beyond $E^*/A=5$ MeV. According to this scenario, contributions from continuum states as high as $E^*/A=8$ MeV are still significant. On the other hand, when the suppression factors $\exp(-t_b/t_i)$ are included (solid lines), the yield peaks at around $E^*/A=4$ MeV and decreases drastically at higher excitation energy due to short lifetime.

To extend continuum states to infinity is impractical. In practice, a cut on the continuum states is made. Figure 2
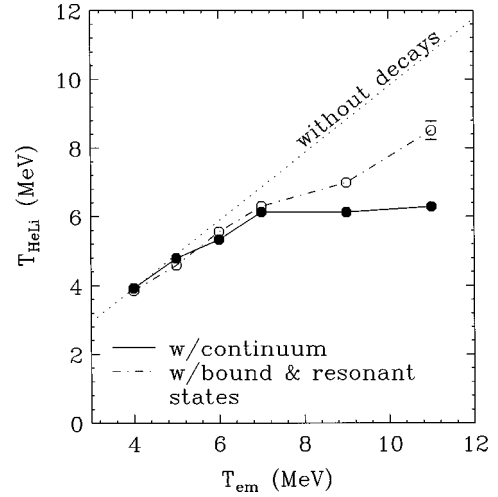
shows the calculated double yield-ratios R_{HeLi} at $T_{em}=7$ MeV (closed circles) and $T_{em}=10$ MeV (open circles) as a function of E_{cut}/A, the energy beyond which the continuum states are not included in the calculations. Above $E_{cut}/A=5$ MeV, the calculated ratio approaches the asymptotic value within the model uncertainty for both emission temperatures. Thus $E_{cut}/A=5$ MeV is chosen as the cutoff energy for continuum states in the present calculations, consistent with the observation shown in the bottom panel of Fig. 1.

Sequential feeding often lowers the apparent temperature. Inclusion of continuum states amplifies this effect. For illustration, we perform sequential calculations for the system Au+Au. The experimental charge distribution of $Z^{2.5}$ at excitation energy of 13.2A MeV [29] was used to constraint the calculation as described in Sec. III. Figure 3 shows the apparent isotope temperature T_{HeLi} as a function of the input (emission) temperature. Sequential decay calculations including only known bound states and resonances are shown by the dot-dashed line. There is a monotonic dependence between T_{HeLi} and T_{em} even though the sensitivity to T_{HeLi} decreases with increasing temperature. For reference, the dotted line represents calculations with no secondary decay. Without the influence of secondary decay, the calculated isotope temperature is nearly the same as the input temperature. However, when continuum states are included, the calculation flattens out at $T_{em}>7$ MeV as shown by the solid line. Inclusion of sequential decay contributions from the continuum enhances decays to low-lying states and renders T_{HeLi} insensitive to the emission temperature at high excitation energy [29,30].

III. EXPERIMENTAL CONSTRAINTS

In the present calculations, μ_p and μ_n in Eq. (1) are not given the values assigned to them as ''chemical potentials'' [31] or ''free excitation energies'' [21] within the specific statistical model. Instead, they are determined from two experimental constraints: the charge-to-mass ratio of the parent nucleus is required to be the same as the charge-to-mass ratio of the emitted charged particles (up to $Z=13$) from the cal-
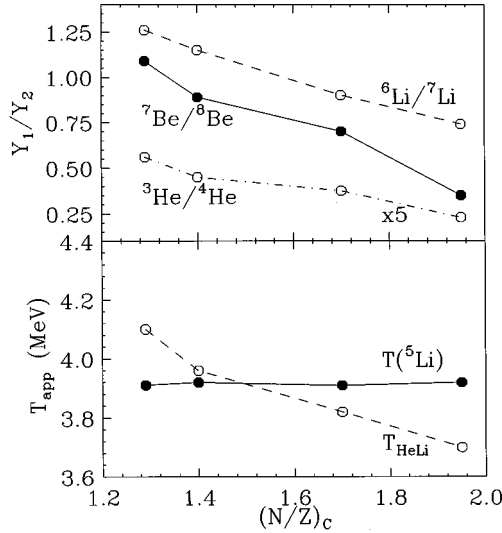
FIG. 4. Apparent temperatures (bottom panel) and single isotope ratios (top panel) plotted as a function of $(N/Z)_C$ used in the sequential decay calculations.

culations, and the final charge distributions reproduce the experimental charge distributions.

A. Effects of charge-to-mass ratio of the emitted particles

If the measured yields were not affected by secondary decay in the thermal model, temperatures from the double isotope ratios obtained from Eq. (4) should be independent of the neutron to proton numbers of the parent nucleus. Since the measured isotope yields are not the same as the primary distribution, this is not necessarily true. If the system breaks up completely into fragments with no residue left, the sum of all the charge of the charged particles divided by the sum of all the neutrons, free and bound, should be equal to the $(N/Z)_C$ of the compound nucleus due to conservation of particle number:

$$(N/Z)_C = \frac{\Sigma m_i N_i}{\Sigma m_i Z_i}, \tag{7}$$

where m_i is the multiplicity of a given isotope and Z_i and N_i are the charge number and neutron number of the emitted particle, respectively. For the Au+Au system, the nominal value of $(N/Z)_C$ is 1.49. In the bottom panel of Fig. 4, the double ratio temperature from the Li and He isotopes T_{HeLi} (dashed line) and temperature from the ^{5}Li excited states and ground states $T(^5\text{Li})$ (solid line) are plotted as a function of $(N/Z)_C$. In all the calculations, T_{em} is set to 4 MeV and the parameters μ_p and μ_n, in Eq. (4) are adjusted to reproduce the charge distribution, $Z^{-2.5}$.

Over the range from $(N/Z)_C = 1.3$ to 2.0, T_{HeLi} changes by more than 10% but $T(^5\text{Li})$ remains constant since temperature deduced from excited states involves only one isotope and is not dependent on $(N/Z)_C$. However, T_{HeLi} changes by less than 5% over the more reasonable values of $(N/Z)_C$ from 1.4 to 1.7. Thus, experimentally, one does not expect to see much variation in the apparent temperature due to isospin effects. On the other hand, changes in $(N/Z)_C$ should affect the single isotope ratio much more. The single
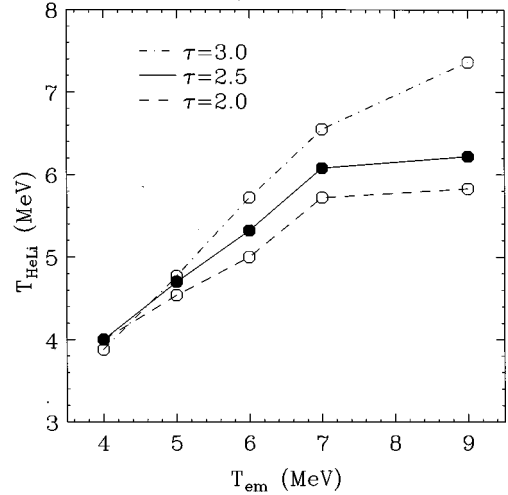

FIG. 5. Calculated T_{HeLi} as a function of input temperatures T_{em} for different charge distribution parameters τ.

isotope yield-ratio $Y(^6\text{Li})/Y(^7\text{Li})$ (dashed line), $Y(^7\text{Be})/Y(^9\text{Be})$ (solid line), and $Y(^3\text{He})/Y(^4\text{He})$ (dot-dashed line) are plotted in the top panel of Fig. 4. The single ratios change by about 50% from $N/Z = 1.3$ to 1.7. Such observation that the single ratios change while the double ratios remain stable has been confirmed recently by studying the singles and double hydrogen and helium isotope ratios of $^{124}\text{Sn}+^{124}\text{Sn}$ and $^{112}\text{Sn}+^{112}\text{Sn}$ reactions at $E/A = 40$ MeV [32].

B. Effects of charge distributions

For most heavy-ion reactions, the experimental charge distribution can be parametrized by the power law $P(Z) \propto Z^{-\tau}$. The effects of sequential decays depend on the primary charge distributions, with steep distributions yielding fewer particles from sequential decays than flat distributions. Before comparing any model predictions to experimental results, it is important that the final charge distributions from the calculations reproduce the experimental distributions. This can be accomplished by adjusting the chemical potential parameters μ_p and μ_n in Eq. (4). To examine the sensitivity of the isotope temperature T_{HeLi} to the charge distribution parameters τ, T_{HeLi} is plotted in Fig. 5 as a function of the emission temperature T_{em} for values of μ_n and μ_p which provide $\tau = 2.0$, 2.5, and 3.0. Below $T_{em} < 5$ MeV, T_{HeLi} is relatively insensitive to τ. In contrast, T_{HeLi} is very sensitive to τ at high emission temperatures. In this region, small uncertainties in τ result in large uncertainties in the extracted isotope temperature. Thus, the experimental uncertainties in τ often preclude the determination of meaningful temperature at high excitation energy [29].

IV. FLUCTUATIONS OF ISOTOPE TEMPERATURES

Following Eq. (2), the isotope temperature can be determined from the yield of ratios of two pairs of isotopes. Within each pair, the two isotopes differ from each other by one neutron number. If there were no influence from the secondary decay, any combination of isotope pairs, i.e., thermometers, fulfilling this condition should yield the same
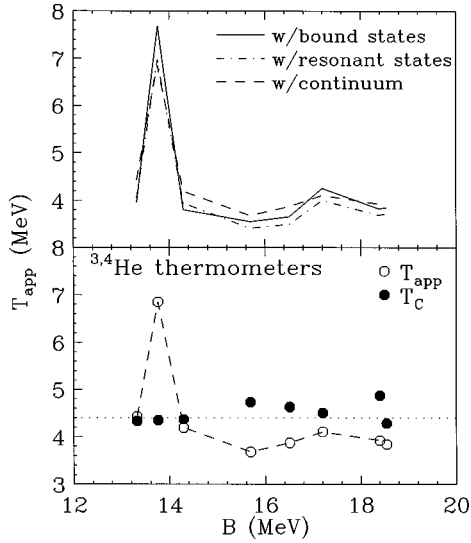
FIG. 6. Calculated T_{app} as a function of binding energy difference B (bottom panel) for isotope ratios involving ^{3}He, ^{4}He listed in Table I. Top panels shows three calculations with different types of excited states included.

TABLE I. List of isotope thermometers involving (^{3}He, ^{4}He) isotope pair with $B > 10$ MeV using the empirical correction factors $\ln \kappa/B$ obtained in Ref. [34].

Isotope ratio	a	B (MeV)	$(\ln \kappa/B)_{expt}$ (MeV^{-1})
(^{6,7}Li, ^{3,4}He)	2.18	13.32	-0.0051
(^{9,10}Be, ^{3,4}He)	0.38	13.76	-0.084
(^{2,3}H, ^{3,4}He)	1.59	14.29	0.0097
(^{12,13}B, ^{3,4}He)	1.95	15.69	0.0601
(^{8,9}Li, ^{3,4}He)	1.24	16.51	0.0423
(^{11,12}B, ^{3,4}He)	1.11	17.20	0.0215
(^{1,2}H, ^{3,4}He)	5.60	18.40	0.0496
(^{7,8}Li, ^{3,4}He)	1.98	18.54	0.0265

temperature. However, recent studies of more than 1300 thermometers reveal that the apparent temperatures are highly dependent on the particular isotopes used [33]. In general, fluctuations arising from different thermometers are largest for those with small values of binding-energy parameter B in Eq. (2).

Thermometers with large B fluctuate less but require one pair of the isotopes used in Eq. (2) to include one strongly bound stable nucleus and one neutron deficit nucleus, so the pair has a large binding energy difference. Since α particles are strongly bound, the isotope pair (^{3}He, ^{4}He) provides many isotope thermometers with $B > 10$ MeV which have been studied extensively in the literature [9–16,18,19]. The (^{11}C, ^{12}C) isotope pair also has a large binding energy difference arising from the strongly bound ^{12}C and the neutron deficit ^{11}C nuclei. Thus, one can form many double isotope yield ratios using (^{11}C, ^{12}C) isotopes [33]. Due to the low cross section and the difficulty in isotope separation, the thermometers involving heavier isotope ratios such as (^{11}C, ^{12}C) have been less studied experimentally [15,33].

The bottom panel of Fig. 6 shows the calculated isotope temperatures of Eq. (2) using isotope ratios listed in Table I, according to increasing B for $T_{em} = 4.4$ MeV. Before sequential decays, the calculated temperatures from primary ground state yields [Eq. (4)] are independent of specific isotope ratios used, at T_{em} as shown by the dotted line. After sequential feedings, the calculated apparent temperatures fluctuate (open points).

The calculated values in Fig. 6 are mostly below 4.4 MeV. The exception is the one involving (^{9}Be, ^{10}Be) ratio whose apparent temperature is above 7 MeV. To show the fluctuations more clearly, dashed lines are drawn to guide the eye. The trends of the fluctuations (high and low values) are similar to those observed experimentally in the central Au+Au collisions at $E/A = 35$ MeV [13].

To study the effects of different contributions from sequential decays to the fluctuations, calculations were performed by including different classes of excited states. The

solid lines in the top panels of Fig. 6 represent apparent temperatures predicted by calculations where only observed discrete bound states [24] are included in the sequential decay calculations. For the He thermometers, when known particle unbound resonances [24] are included, the fluctuations change slightly (dot-dashed lines). Finally, when contributions from the higher states in the continuum as described in Sec. II, are included, there are slightly more changes (dashed lines).

Similar studies have been performed for the thermometers involving (^{11}C, ^{12}C) as shown in Fig. 7. Compared to He thermometers, the effects of including more states are much larger. For example, most of the (^{11}C, ^{12}C) thermometers calculated from sequential decays including bound states only (solid line, upper panel) are a few MeV higher than the temperatures including more states. The effect of inclusion of known particle unbound resonances (dot-dashed lines) and states in the continuum (dashed lines) lower the temperature to around 3 MeV, much below the input temperature of 4.4 MeV. [In many experimental measurements, the (^{11}C, ^{12}C) thermometers provide apparent temperatures around 4 MeV, somewhat higher than these illustrative results.]

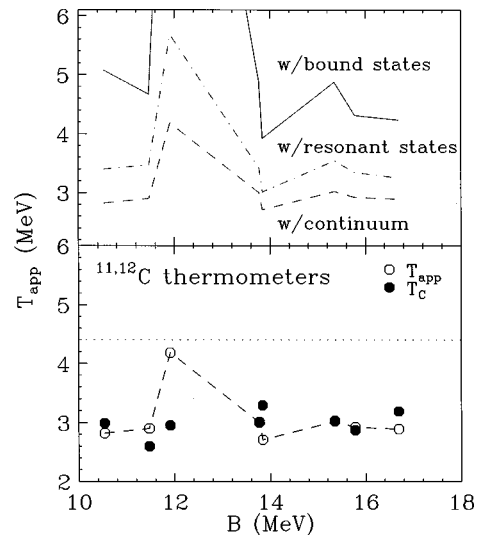It is not clear why the current model fails to predict the

FIG. 7. Calculated T_{app} as a function of binding energy difference B (bottom panel) for isotope ratios involving (^{11}C, ^{12}C) listed in Table II.

carbon temperatures. One problem is the inability of the current calculations to predict the carbon isotope distributions [5,6]. The calculated distributions are much narrower than the experimental ones. In addition, the model tends to over-predict the number of particles decaying to the ground state of the stable and neutron rich nuclei such as ^{12}C, ^{13}C and severely under-predicts the yield of neutron deficit nuclei such as ^{11}C. More work is clearly needed to understand the effect of sequential decays on the temperatures extracted from these heavy isotopes.

Recently, empirical sequential decay corrections have been used to relate the apparent temperatures to the freeze-out temperatures T_0

$$\frac{1}{T} = \frac{1}{T_0} + \frac{\ln \kappa}{B}, \tag{8}$$

where the measured ratio R (after sequential decay) is assumed to be proportional to the ratio obtained from the primary ground state yields R_0

$$R = \kappa R_0. \tag{9}$$

The values of $\ln \kappa/B$ have been determined experimentally for some isotope ratios by assuming T_0 to be the temperatures determined from excited states [33,34]. These correction factors obtained at temperature around 4 MeV are found to reduce the fluctuations in the apparent temperatures in general. To the first order, the experimentally observed $\ln \kappa/B$ values obtained at temperature around 4 MeV, are found to be independent of the reactions and excitation energies.

To investigate the properties of these correction factors, we applied the empirical determined $\ln \kappa/B$ values listed in Tables I and II to the calculated temperatures shown in the bottom panels of Figs. 6 and 7. Due to the large number of low-lying states in ^{10}Be, any isotope ratios including ^{9}Be/^{10}Be yield ratios exhibit large apparent temperatures. By applying Eq. (8), this temperature normally decreases to values comparable to other isotope ratios. In the case of (^{3}He, ^{4}He) thermometers, the empirical correction factors of $\ln \kappa/B$ listed in Refs. [33, 34] account for most of the fluctuations and bring the corrected temperatures (solid circles)

TABLE II. List of isotope thermometers involving (^{11}C, ^{12}C) isotope pair with $B > 10$ MeV using the empirical correction factors $\ln \kappa/B$ obtained in Ref. [33].

Isotope ratio	a	B (MeV)	$(\ln(\kappa)/B)_{\text{expt}}$ (MeV^{-1})
^{13,14}C/^{11,12}C	1.96	10.54	0.021
^{6,7}Li/^{11,12}C	5.90	11.47	-0.039
^{9,10}Be/^{11,12}C	1.03	11.91	-0.098
^{12,13}C/^{11,12}C	7.92	13.77	0.0015
^{12,13}B/^{11,12}C	5.28	13.84	0.065
^{11,12}B/^{11,12}C	3.00	15.35	0.010
^{8,9}Li/^{11,12}C	3.35	15.78	-0.006
^{7,8}Li/^{11,12}C	5.36	16.69	0.033

in agreement with the input temperature (dotted line). However, for (^{11}C, ^{12}C) thermometers, except for the ratios involving ^{9}Be/^{10}Be, the sequential decay correction factors affect the raw temperatures little and the corrected temperature cluster around 3 MeV instead of 4.4 MeV, the input temperature of the calculations. Without additional information, such as calibrations from other thermometers, it is not clear the mean corrected isotope temperatures obtained from Eq. (8) using the $\ln \kappa/B$ values of Tables I and II give the freeze-out temperatures.

V. SUMMARY

In summary, sequential decay calculations that include bound states, known resonant states, and continuum states were studied. Unlike other statistical models where temperature and density were the model input parameter, we performed the calculation for a particular set of experimental data by changing emission temperature and require that the charge distribution be reproduced by calculation. Our calculation indicates that due to a strong feeding effect, especially from continuum states, nuclear temperature measurements from the double isotope ratio at temperatures beyond 6 MeV are strongly affected by secondary decays. The fluctuations between different isotope thermometers observed in the experiment are mainly due to structure effects in the secondary decay process.

[1] J. Pochodzalla, W. A. Friedman, C. K. Gelbke, W. G. Lynch, M. Maier, D. Ardouin, H. Delagrange, H. Doubre, C. Grégoire, A. Kyanowski, W. Mittig, A. Péghaire, J. Péter, F. Saint-Laurent, Y. P. Viyogi, B. Zwieglinski, G. Bizard, F. Lefèbvres, B. Tamain, and J. Québert, Phys. Rev. Lett. **55**, 177 (1985).

[2] J. Pochodzalla, C. K. Gelbke, W. G. Lynch, M. Maier, D. Ardouin, H. Delagrange, H. Doubre, C. Grégoire, A. Kyanowski, W. Mittig, A. Péghaire, J. Péter, F. Saint-Laurent, B. Zwieglinski, G. Bizard, F. Lefèbvres, B. Tamain, J. Québert, Y. P. Viyogi, W. A. Friedman, and D. H. Boal, Phys. Rev. C **35**, 1695 (1987).

[3] Z. Chen, C. K. Gelbke, W. G. Gong, Y. D. Kim, W. G. Lynch, M. R. Maier, J. Pochodzalla, M. B. Tsang, F. Saint-Laurent, D.

Ardouin, H. Delagrange, H. Doubre, J. Kasagi, A. Kyanowski, A. Péghaire, J. Péter, E. Rosato, G. Bizard, F. Lefèbvres, B. Tamain, J. Québert, and Y. P. Viyogi, Phys. Rev. C **36**, 2297 (1987).

[4] Z. Chen and C. K. Gelbke, Phys. Rev. C **38**, 2630 (1988).

[5] H. M. Xu, W. G. Lynch, C. K. Gelbke, M. B. Tsang, D. J. Fields, M. R. Maier, D. J. Morrissey, T. K. Nayak, J. Pochodzalla, D. G. Sarantites, L. G. Sobotka, M. L. Halbert, and D. C. Hensley, Phys. Rev. C **40**, 186 (1989).

[6] T. K. Nayak, T. Murakami, W. G. Lynch, K. Swartz, D. J. Fields, C. K. Gelbke, Y. D. Kim, J. Pochodzalla, M. B. Tsang, H. M. Xu, F. Zhu, and K. Kwiatkowski, Phys. Rev. C **45**, 132 (1992).

[7] C. Schwarz, W. G. Gong, N. Carlin, C. K. Gelbke, Y. D. Kim,

W. G. Lynch, T. Murakami, G. Poggi, R. T. de Souza, M. B. Tsang, H. M. Xu, D. E. Fields, K. Kwiatkowski, V. E. Viola, Jr., and S. J. Yennello, Phys. Rev. C **48**, 676 (1993).

[8] F. Zhu, W. G. Lynch, D. R. Bowman, R. T. de Souza, C. K. Gelbke, Y. D. Kim, L. Phair, M. B. Tsang, C. Williams, and H. M. Xu, Phys. Rev. C **52**, 784 (1995).

[9] H. Xi, Zhan Wenlong, Zhu Yongtai, Guo Zhongyan, Hu Xiao-qing, Liu Guanhua, Zhou Jianqun, Yin Shuzhi, Zhao Youxiong, Wei Zhiyong, and Fan Enjie, Nucl. Phys. **A552**, 281 (1993).

[10] S. Albergo, S. Costa, E. Costanza, and A. Rubbino, Nuovo Cimento A **89**, 1 (1985).

[11] J. Pochodzalla, T. Möhlenkamp, T. Rubehn, A. Schüttauf, A. Wörner, E. Zude, M. Begemann-Blaich, Th. Blaich, H. Emling, A. Ferrero, C. Gross, G. Immé, I. Iori, G. J. Kunde, W. D. Kunze, V. Lindenstruth, U. Lynen, A. Moroni, W. F. J. Müller, B. Ocker, G. Raciti, H. Sann, C. Schwarz, W. Seidel, V. Serfling, J. Stroth, W. Trautmann, A. Trzcinski, A. Tucholski, G. Verde, and B. Zwieglinski, Phys. Rev. Lett. **75**, 1040 (1995).

[12] V. Serfling, C. Schwarz, R. Bassini, M. Begemann-Blaich, S. Fritz, S. J. Gaff, C. Groß, G. Immé, I. Iori, U. Kleinevoß, G. J. Kunde, W. D. Kunze, U. Lynen, V. Maddalena, M. Mahi, T. Möhlenkamp, A. Moroni, W. F. J. Müller, C. Nociforo, B. Ocker, T. Odeh, F. Petruzzelli, J. Pochodzalla, G. Raciti, G. Riccobene, F. P. Romano, A. Saija, M. Schnittker, A. Schüttauf, W. Seidel, C. Sfienti, W. Trautmann, A. Trzcinski, G. Verde, A. Wörner, Hongfei Xi, and B. Zwieglinski, Phys. Rev. Lett. **80**, 3928 (1998).

[13] M. J. Huang, H. Xi, W. G. Lynch, M. B. Tsang, J. D. Dinius, S. J. Gaff, C. K. Gelbke, T. Glasmacher, G. J. Kunde, L. Martin, C. P. Montoya, and E. Scannapieco, P. M. Milazzo, M. Azzano, G. V. Margagliotti, R. Rui, G. Vannini, N. Colonna, L. Celano, G. Tagliente, M. D'Agostino, M. Bruno, M. L. Fiandri, F. Gramegna, A. Ferrero, I. Iori, A. Moroni, F. Petruzzelli, and P. F. Mastinu, Phys. Rev. Lett. **78**, 1648 (1997).

[14] Y.-G. Ma, A. Siwek, J. Péter, F. Gulminelli, R. Dayras, L. Nalpas, B. Tamain, E. Vient, G. Auger, Ch. O. Bacri, J. Benlliure, E. Bisquer, B. Borderie, R. Bougault, R. Brou, J. L. Charvet, A. Chbihi, J. Colin, D. Cussol, E. De Filippo, A. Demeyer, D. Doré, D. Durand, P. Ecomard, P. Eudes, E. Gerlic, D. Gourio, D. Guinet, R. Laforest, P. Lautesse, J. L. Laville, L. Lebreton, J. F. Lecolley, A. Le Févre, T. Lefort, R. Legrain, O. Lopez, M. Louvel, J. Lukasik, N. Marie, V. Métivier, A. Ouatizerga, M. Parlog, E. Plagnol, A. Rahmani, T. Reposeur, M. F. Rivet, E. Rosato, F. Saint-Laurent, M. Squalli, J. C. Steckmeyer, M. Stern, L. Tassan-Got, C. Volant, and J. P. Wieleczko, Phys. Lett. B **390**, 41 (1997).

[15] A. Kolomiets, E. Ramakrishnan, H. Johnston, F. Gimeno-Nogues, B. Hurst, D. O'Kelly, D. J. Rowland, S. Shlomo, T. White, J. Winger, and S. J. Yennello, Phys. Rev. C **54**, R472 (1996).

[16] H. Xi, T. Odeh, R. Bassini, M. Begemann-Blaich, A. S. Botvina, S. Fritz, S. J. Gaff, C. Groß, G. Immé, I. Iori, U. Kleinevoß, G. J. Kunde, W. D. Kunze, U. Lynen, V. Maddalena, M. Mahi, T. Möhlenkamp, A. Moroni, W. F. J. Müller, C. Nociforo, B. Ocker, F. Petruzzelli, J. Pochodzalla, G. Raciti, G. Riccobene, F. P. Romano, Th. Rubehn, A. Saija, M. Schnittker, A. Schüttauf, C. Schwarz, W. Seidel, V. Serfling, C. Sfienti, W. Trautmann, A. Trzcinski, G. Verde, A. Wörner, and B. Zwieglinski, Z. Phys. A **359**, 397 (1997).

[17] D. Hahn and H. Stöcker, Nucl. Phys. **A476**, 718 (1988).

[18] Z. Majka, P. Staszel, J. Cibor, J. B. Natowitz, K. Hagel, J. Li, N. Mdeiwayeh, R. Wada, and Y. Zhao, Phys. Rev. C **55**, 2991 (1997).

[19] F. Gulminelli and D. Durand, Nucl. Phys. **A615**, 117 (1997).

[20] V. Weisskopf, Phys. Rev. **52**, 295 (1937).

[21] W. A. Friedman and W. G. Lynch, Phys. Rev. C **28**, 16 (1983).

[22] J. Bondorf, R. Donangelo, I. N. Mishustin, and H. Schulz, Nucl. Phys. **A444**, 460 (1985).

[23] D. H. E. Gross, Rep. Prog. Phys. **53**, 605 (1990).

[24] F. Ajzenberg-Selove, Nucl. Phys. **A392**, 1 (1983); **A413**, 1 (1984); **A433**, 1 (1985); **A449**, 1 (1985); **A460**, 1 (1986).

[25] W. Hauser and H. Feshbach, Phys. Rev. **87**, 366 (1952).

[26] A. Gilbert and G. W. Cameron, Can. J. Phys. **43**, 1446 (1965).

[27] E. Cornell, T. M. Hamilton, D. Fox, Y. Lou, R. T. de Souza, M. J. Huang, W. C. Hsi, C. Schwarz, C. Williams, D. R. Bowman, J. Dinius, C. K. Gelbke, T. Glasmacher, D. O. Handzy, M. A. Lisa, W. G. Lynch, G. F. Peaslee, L. Phair, M. B. Tsang, G. VanBuren, R. J. Charity, L. G. Sobotka, and W. A. Friedman, Phys. Rev. Lett. **75**, 1475 (1995), and references therein.

[28] M. G. Mustafa, M. Blann, A. V. Ignatyuk, and S. M. Grimes, Phys. Rev. C **45**, 1078 (1992).

[29] H. Xi, W. G. Lynch, M. B. Tsang, and W. A. Friedman, Phys. Rev. C **54**, R2163 (1996).

[30] M. B. Tsang, F. Zhu, W. G. Lynch, A. Aranda, D. R. Bowman, R. T. de Souza, C. K. Gelke, Y. D. Kim, L. Phair, S. Pratt, C. Williams, H. M. Xu, and W. A. Friedman, Phys. Rev. C **53**, R1057 (1996).

[31] D. H. E. Gross, L. Satpathy, Meng Ta-Ching, M. Satpathy, Z. Phys. A **309**, 41 (1982).

[32] G. J. Kunde, S. Gaff, C. K. Gelbke, T. Glasmacher, M. J. Huang, R. Lemmon, W. G. Lynch, L. Manduci, L. Martin, M. B. Tsang, W. A. Friedman, J. Dempsey, R. J. Charity, L. G. Sobotka, D. K. Agnihotri, B. Djerroud, W. U. Schrsder, W. Skulski, and J. Toke, Phys. Lett. B **416**, 56 (1998).

[33] M. B. Tsang, W. G. Lynch, H. Xi, and W. A. Friedman, Phys. Rev. Lett. **78**, 3836 (1997).

[34] H. F. Xi, M. B. Tsang, M. J. Huang, W. G. Lynch, J. D. Dinius, S. J. Gaff, C. K. Gelbke, T. Glasmacher, G. J. Kunde, L. Martin, C. P. Montoya, M. Azzano, G. V. Margagliotti, P. M. Milazzo, R. Rui, G. Vannini, L. Celano, N. Colonna, and G. Tagliente, M. D'Agostino, M. Bruno, M. L. Fiandri, F. Gramegna, A. Ferrero, I. Iori, A. Moroni, F. Petruzzelli, and P. F. Mastinu, Phys. Lett. B **431**, 8 (1998).